P-47

(Final report submitted to NASA-Langley Research Center under
Grant NAG-1-286 to the
University of Illinois at Urbana-Champaign, IL)

Analysis of Delamination in Fiber Composite Laminates Out-of-Plane under Bending

by

S. S. Wang* and F. G. Yuan+
National Center for Composite Materials Research
College of Engineering
University of Illinois
Urbana, IL 61801

---

* Professor and Director

\+ Post-doctoral Research Associate

1. Introduction

Delamination in the form of cracking or separation between plies in an advanced fiber composite laminate has been a problem of major concern. Delaminations are recognized to result from manufacturing/processing defects as well as from high, local interlaminar stresses at geometric boundaries or under impact. The presence of a delamination and its growth may have significant effects on mechanical response and load-bearing capacity of the composite laminate. A delamination may reduce local stiffness structure and, in many cases, lead to premature failure of a composite structure due to local buckling and/or appreciable crack growth. This situation is most critical when a delamination in a composite laminate is subjected to out-of-plane loading, such as bending and torsion. A rigorous study of the delamination problem for a fiber composite under out-of-plane bending is recognized to be difficult. The difficulty is caused by various complexities involved , such as inherent multiphase material system, significant anistropy of the composite, discontinuous mechanical properties through the laminate thickness direction, a large number of lamination parameters, and associated crack-tip stress singularity.

Extensive research efforts have been made on the delamination mechanics problem of a composite laminate subjected to in-plane tensile or compressive loading, for example [1-5]. Interlaminar stresses are found to be dominant in governing the initiation and growth of the composite laminate under an in-plane nominal stress. It is recognized that the interlaminar stresses are more prevalent in a fiber composite laminate subjected to out-of-plane bending [6] than that to in-plane stretching. Consequently, a delamination in a fiber composite laminate subject to bending would experience more significant influence by the presence of the interlaminar stresses. Accurate determination of the magnitude and distribution of interlaminar stresses becomes critical. Attempts on analytical evaluation of the delamination behavior in a composite laminate have been extremely limited [7], because of the difficulties in accurately determining the complex interlaminar stresses and deformation. It is not surprising to recognize this difficulty since interlaminar stress and

deformation are generally three-dimensional in nature. The local crack-tip response associated with a delamination requires simultaneous evaluation of the coupled mode-I, II and III fracture mechanics parameters. However, in order to have a clear understanding of the delamination problems in a composite material under bending, an accurate solution obtained based on the 3-D (or quasi-3-D) laminate elasticity theory and the recently developed composite fracture mechanics analysis is essential. Both quasi three-dimensional solutions and fully 3-D solutions are considered to be critical to the advancement of analysis and design of composite materials in the future. Also, with the aid of the recently developed laminate elasticity for fiber composites, it becomes possible to look rigorously into the delamination problem in a composite laminate under bending.

The objectives of this paper are to: (1) develop an asymptotic solution for a composite laminate subjected to out-of-plane bending, (2) construct advanced singular finite elements in conjunction with the developmenmt of nonsingular elements for this bending problem, (3) evaluate the delamination failure mechanics parameters and the subsequent modes of fracture. Both advanced analytical methods and advanced computational analyses are conducted to realize these goals. A parametric study was also conducted to evaluate the influences of various lamination parameters on the delaminated composites.

In the next section, basic formulation of laminate elasticity is given and governing partial differential equations of the delamination problem are established. Also, the general solution structure is determined by an eigenfunction expansion method. In Section 3, advanced numerical methods are introduced to formulate singular, local crack-tip elements and the nonsingular elements in the surrounding area in a delaminated composite. The fracture mechanics parameters, such as delamination crack-tip stress intensity factors and energy release rates, for the problem is addressed in Section 4. Numeral results are obtained for various cases of interest in Section 5. Important problem parameters, such as the size of the singular element, the effect of delamination length and fiber orientation as well as the laminate layup, are studied to examine the fundamental nature of the solution method and the delamination crack-tip field. The effect of delamination location, i.e.,

edge delamination and center delamination, on the local fracture is examined in Section 5. Conclusions derived from this study is given in Section 6.

2.1 Basic Formulation

Consider a composite laminate composed of fiber-reinforced composite plies subjected to an applied nominal end bending moment per unit width, M_x^∞, as shown in Fig. 1. Let V denote the interior of a composite laminate of length 2L and a cross section B with the lateral boundary ∂B. The Cartesian coordinates are chosen such that the z-axis is the generator of B. The end cross sections are denoted by Σ_1 and Σ_2, respectively, and located at z = -L and z = L. The constitutive equations of each individual composite ply are denoted by generalized Hooke's law in contracted notation as

$$\varepsilon_i = S_{ij}\,\sigma_j, \qquad (i, j = 1,2,3,...,6) \tag{2.1}$$

where repeated subscripts indicate summation, and S_{ij} is the compliance tensor. The engineering strains, ε_i, in Eq. (2.1) are defined by

$$\varepsilon_1 = \varepsilon_x = \frac{\partial u}{\partial x}, \quad \varepsilon_2 = \varepsilon_y = \frac{\partial v}{\partial y}, \quad \varepsilon_3 = \varepsilon_z = \frac{\partial w}{\partial z},$$
$$\varepsilon_4 = 2\gamma_{yz} = \frac{\partial w}{\partial y} + \frac{\partial v}{\partial z}, \quad \varepsilon_5 = 2\gamma_{xz} = \frac{\partial w}{\partial x} + \frac{\partial u}{\partial z}, \quad \varepsilon_6 = 2\gamma_{xy} = \frac{\partial u}{\partial y} + \frac{\partial v}{\partial x} \tag{2.2}$$

where u, v and w are displacement components. The stresses, σ_i, are defined in an analogous manner.

The composite laminate is assumed to be sufficiently long that in the region far from the end, the end effect is neglected by virtue of Saint-Venant's Principle. Thus in this generalized plane deformation problem [8], stresses in the laminate are independent of the z-coordinate. Under these assumptions, equations of equilibrium without body force lead to

$$\frac{\partial \sigma_x}{\partial x} + \frac{\partial \tau_{xy}}{\partial y} = o,$$
$$\frac{\partial \tau_{xy}}{\partial x} + \frac{\partial \sigma_y}{\partial y} = o, \qquad (2.3)$$
$$\frac{\partial \tau_{xz}}{\partial x} + \frac{\partial \tau_{yz}}{\partial y} = o$$

Integrating Eq. (2.1) with the aid of Eq. (2.2), one can obtain u, v and w as

$$u = -\frac{z^2}{2}\frac{\partial D}{\partial x} + (S_{5j}\sigma_j - \frac{\partial w_o}{\partial x})\, z + U_o(x,y)$$
$$v = -\frac{z^2}{2}\frac{\partial D}{\partial y} + (S_{4j}\sigma_j - \frac{\partial w_o}{\partial y})\, z + V_o(x,y) \qquad (2.4)$$
$$w = Dz + W_o(x,y)$$

where $D = S_{3j}\,\sigma_j$, and U_o, V_o, and W_o are arbitrary functions of x and y only. (2.5)

Following the procedure in [9], it can be easily shown that general expressions for the displacements and the stress component σ_z have the following form:

$$u(x,y,z) = -\frac{1}{2} A_1 S_{33} z^2 - A_4 yz + U(x,y)$$
$$v(x,y,z) = -\frac{1}{2} A_2 S_{33} z^2 + A_4 xz + V(x,y) \qquad (2.6)$$
$$w(x,y,z) = (A_1 x + A_2 y + A_3) S_{33} z + W(x,y)$$
$$\sigma_z = A_1 x + A_2 y + A_3 - S_{3j}\sigma_j / S_{33}, \qquad (j=1,2,4,5,6)$$

where A_1 and A_2 pertain to the external bending on the composite laminate, acting in the x-z and y-z planes. The A_3 characterizes uniform axial extension of the composite, and A_4, the relative angle of rotation about the z-axis.

The unknown functions, U, V, and W, depend on x and y only, and can be easily shown to obey the following relationships:

$$\frac{\partial U}{\partial x} = \tilde{S}_{1j}\,\sigma_j + S_{13}\,(A_1 x + A_2 y + A_3)$$
$$\frac{\partial V}{\partial y} = \tilde{S}_{2j}\,\sigma_j + S_{23}\,(A_1 x + A_2 y + A_3)$$
$$\frac{\partial W}{\partial x} = \tilde{S}_{3j}\,\sigma_j + S_{53}\,(A_1 x + A_2 y + A_3) + A_4 y \qquad (2.7)$$

$$\frac{\partial W}{\partial y} = \tilde{S}_{4j}\,\sigma_j + S_{43}\,(A_1 x + A_2 y + A_3) - A_4 x$$

$$\frac{\partial U}{\partial y} + \frac{\partial V}{\partial x} = \tilde{S}_{2j}\,\sigma_j + S_{63}\,(A_1 x + A_2 y + A_3),$$

$$(j = 1,2,4,5 \text{ and } 6)$$

where $\tilde{S}_{ij} = S_{ij} - S_{i3}\,S_{j3}/S_{33}.$ (2.8)

Applying the interface continuity conditions, $\underset{\sim}{u}^{(m)} = \underset{\sim}{u}^{(m+1)}$, between the m-th and (m + 1)th plies leads to the following relationships for A_i:

$$A_i^{(m)}\ S_{33}^{(m)} = A_i^{(m+1)}\ S_{33}^{(m+1)}, \qquad (2.9)$$

$$A_4^{(m)} = A_4^{(m+1)}, \qquad (i = 1,2,3).$$

Traction-free boundary conditions on the lateral boundary ∂B satisfy the following expressions:

$$\begin{aligned} &\sigma_x\, n_x + \tau_{xy}\ n_y = 0, \\ &\tau_{xy}\, n_x + \sigma_y\ n_y = 0, \\ &\tau_{xz}\, n_x + \tau_{yz}\ n_y = 0, \end{aligned} \qquad (2.10)$$

where n_x and n_y are outward unit normal of ∂B.

The end loading conditions on the laminate cross-section Σ_i under the present bending M_x^∞, have the form obtainable from statically equivalent loads as

$$\begin{aligned} &\iint_{\Sigma_i} \tau_{xz}\,dxdy = 0, \qquad \iint_{\Sigma_i} \tau_{yz}\,dxdy = 0 \\ &\iint_{\Sigma_i} \tau_z\,dxdy = 0 \\ &\iint_{\Sigma_i} \tau_{xy}\,dxdy = M_x^\infty \\ &\iint_{\Sigma_i} \tau_{yz}\,dxdy = 0 \qquad (i = 1,2) \\ &\iint_{\Sigma_i} (\tau_{yzx} - \tau_{xzy})\,dxdy = 0 \end{aligned} \qquad (2.11)$$

2.2 Governing Partial Differential Equations

Introducing stress functions F(x,y) and ψ (x,y) such that

$$\sigma_x = \frac{\partial^2 F}{\partial y^2}, \quad \sigma_y = \frac{\partial^2 F}{\partial x^2}, \quad \tau_{xy} = - \frac{\partial^2 F}{\partial x \partial y},$$
$$\tau_{xz} = \frac{\partial \psi}{\partial y}, \quad \tau_{yz} = - \frac{\partial \psi}{\partial x}, \tag{2.12}$$

the equations of equilibrium can be satisfied identically. Eliminating U and V from Eqs. (2.7) by differentiation, one obtains the following system of coupled governing partial differential equations for this problem:

$$L_3 F + L_2 \psi = -2A_4 + A_1 S_{34} - A_2 S_{35},$$
$$L_4 F + L_3 \psi = 0. \tag{2.13}$$

where L_2, L_3, and L_4 are linear differential operators defined in [9]

$$L_2 = \tilde{S}_{44} \frac{\partial^2}{\partial x^2} - 2\tilde{S}_{45} \frac{\partial^2}{\partial x \partial y} + \tilde{S}_{55} \frac{\partial^2}{\partial y^2}$$

$$L_3 = \tilde{S}_{24} \frac{\partial^3}{\partial x^3} + (\tilde{S}_{25} + \tilde{S}_{46}) \frac{\partial^3}{\partial x^2 \partial z} - (\tilde{S}_{14} + \tilde{S}_{56}) \frac{\partial^3}{\partial x \partial y^2} + \tilde{S}_{15} \frac{\partial^3}{\partial y^3} \tag{2.14}$$

$$L_4 = \tilde{S}_{22} \frac{\partial^4}{\partial x^4} - 2\tilde{S}_{26} \frac{\partial^4}{\partial x^3 \partial y} + (2\tilde{S}_{12} + \tilde{S}_{46}) \frac{\partial^4}{\partial x^2 \partial y^2} - 2\tilde{S}_{16} \frac{\partial^4}{\partial x \partial y^3} + \tilde{S}_{11} \frac{\partial^4}{\partial y^4}$$

2.3 General Solution Structure

The governing equations Eqs. (2.13), are coupled linear partial differential equations with constant coefficients related to elastic constants of each composite lamina. The complete solution for Eqs. (2.13) consists of a homogeneous solution and a particular solution. Lehknitskii has shown [8] that the homogeneous solution for the above system of governing partial differential equations has the general form

$$F(x,y) = \sum_{k=1}^{6} F_k (x + \mu_k y), \tag{2.15a}$$

$$\psi(x,y) = \sum_{k=1}^{6} \eta_k F_k'(x + \mu_k y) \tag{2.15b}$$

where the prime (') in Eqs. (2.15) denotes differentiation of the function $F_k(x + \mu_k y)$ with respect to its argument. The coefficients μ_k are the roots of following characteristic algebraic equation:

$$l_4(\mu)\ l_2(\mu)\ -\ l_3^2(\mu) = 0$$

where

$$\begin{aligned} l_2(\mu) &= \tilde{S}_{55}\mu^2 - \tilde{S}_{45}\mu^2 + \tilde{S}_{44} \\ l_3(\mu) &= \tilde{S}_{15}\mu^3 - (\tilde{S}_{14} + \tilde{S}_{56})\mu^2 + (\tilde{S}_{25} + \tilde{S}_{46})\mu - \tilde{S}_{24} \\ l_4(\mu) &= \tilde{S}_{11}\mu^4 - 2\tilde{S}_{16}\mu^3 + (2\tilde{S}_{12} + \tilde{S}_{66})\mu^2 - 2\tilde{S}_{26}\mu + \tilde{S}_{22} \end{aligned} \tag{2.16}$$

It can be shown that μ_k cannot be real and have to appear as complex conjugates. Thus F_k are analytic functions of the complex variables $Z_k = x + \mu_k y$. The general solutions for stress and displacement are constructed in the form as

$$\begin{aligned} \sigma_i &= \sigma_i^{(h)} + \sigma_i^{(p)}, \qquad (i = 1,2,....,6) \\ u_j &= u_j^{(h)} + u_j^{(p)} \qquad (j = 1,2,3) \end{aligned} \tag{2.17}$$

The homogeneous components of the stress and the displacement solutions can be expressed in terms of $F_k(Z_k)$ as

$$\begin{aligned} \sigma_x^{(h)} &= \sum_{k=1}^{6} \mu_k F_k''(Z_k), \quad \sigma_y^{(h)} = \sum_{k=1}^{6} F_k''(Z_k) \\ \tau_{yz}^{(h)} &= \sum_{k=1}^{6} \eta_k F_k''(Z_k), \quad \tau_{xz}^{(h)} = \sum_{k=1}^{6} \mu_k \eta_k F_k''(Z_k) \\ \tau_{xy}^{(h)} &= \sum_{k=1}^{6} \mu_k F_k''(Z_k) \end{aligned} \tag{2.18}$$

$$u^{(h)} = \sum_{k=1}^{6} p_k F_k'(Z_k), \qquad v^{(h)} = \sum_{k=1}^{6} q_k F_k'(Z_k),$$

$$w^{(h)} = \sum_{k=1}^{6} t_k F_k'(Z_k). \tag{2.19}$$

where p_k, q_k and t_k are known constants with their expressions defined in [8].

The $\sigma_i^{(p)}$ and $u_j^{(p)}$ are particular solutions for the problem, depending upon the loading mode, composite lamination parameters and geometric variables of the composite. The particular solutions for σ_i and u_j can be found by various analytical and numerical methods, dependent upon the complexity of the problem.

An appropriate form of $F_k(Z_k)$ has been suggested in [9].

$$F_k(Z_k) = C_k Z_k^{(\delta+2)} / [(\delta+1)(\delta+2)] \tag{2.20}$$

where C_k and δ are complex constants to be determined later. Substituting Eq. (2.20) into Eqs. (2.18) and (2.19), one can express $\sigma_i^{(h)}$ and $u_j^{(h)}$ in terms of δ, C_k and Z_k.

The homogeneous solutions for the stress and displacement shown in Eqs. (2.18) and (2.19) are required to satisfy the near-field boundary conditions and interface continuity conditions, leading to a standard eigenvalue problem in the form of a transcendental equation for determining the values of δ. After the eigenvalues, δ, are determined, the stress and displacement may be expressed as

$$\sigma_i^{(h)} = \sum_{m=1}^{\infty} \sum_{k=1}^{\infty} d_m \, f_{im}(Z_k;\delta_m)$$

$$u_j^{(h)} = \sum_{m=1}^{\infty} \sum_{k=1}^{\infty} d_m \, g_{jm}(Z_k;\delta_m) \tag{2.21}$$

where the d_m are unknown constants and f_{im} and g_{jm} denote the known eigenfunctions corresponding to the m-th eigenvalue δ_m.

The particular solutions for the stress and displacement in the present delamination problem of a composite laminate under out-of-plane bending are extremely complex and difficult to be obtained analytically in a closed form due to complex geometry of the crack, the laminate parameters and the out-of-plane loading mode. An advanced numerical method is developed in conjunction with the asymptotic solution obtained here to give the full-field solution for the problem.

3. Numerical Methods

Owing to the complex nature of the problem, a closed-form full-field solution for the delamination problem in a fiber composite laminate under out-of-plane bending is difficult to obtain, especially the determination of the particular solution. Advanced numerical methods are introduced here to account for the various difficulties and to obtain the full-field solution. Based on the asymptotic solution determined in the previous section, a singular delamination crack-tip element is formulated. Also, based on the laminate elasticity field equations, a compatible non-singular surrounding element is constructed for the bending problem of a delaminated composite laminate.

3.1 Near-Field Element Formulation

In the previous studies [10,11,12], the detailed nature of the composite delamination crack-tip singularity has been examined. For a delamination with a closed crack tip with frictionless crack surface contact, an inverse square-root singularity has been determined [12]. Also, for an open delamination crack tip and for a crack with a small amount of crack closure, asymptotic solutions with an inverse-square root stress singularity are also approximated [11]. Based on these results, the delamination crack-field solution structure can be properly constructed. In order to include the local stress singularity, the element formulation introduced by Stern[13] is employed. The element is a six-node triangular element in which the assumed displacement field contains terms proportional to the square root of distance along lines emanating from the crack tip. The element is fully compatible with the neighboring isoparametric quadratic elements.

Nodal arrangements and element configurations for the present problem are shown in Fig. 2 with the node 1 being singular. Transformation is needed for the triangular polar coordinates (ρ,ξ) to the global Cartesian coordinates (x,y,z). Coordinates of any given point in the element are given by

$$\underset{\sim}{x} = \underset{\sim}{x}_1 + \rho \{ (\underset{\sim}{x}_2 - \underset{\sim}{x}_1) + \xi (\underset{\sim}{x}_3 - \underset{\sim}{x}_2) \}. \tag{3.1}$$

where $\underset{\sim}{x}_i$ (i=1,2,3) are global Cartesian coordinates of the vertices of the singular element. Furthermore, the relationships between the spatial polar coordinates (r,θ) with the origin at node 1 and the triangular polar coordinates (ρ,ξ) are

$$r = R(\xi)\,\rho, \qquad \theta = \Theta(\xi). \tag{3.2}$$

where $R(\xi) = \{ (x_2 - x_1)^2 + (y_2 - y_1)^2 + 2\xi [(x_2 - x_1)(x_3 - x_2) + (y_2 - y_1)(y_3 - y_2)] + \xi^2 [(x_1 - x_2)^2 + (y_3 - y_2)^2]\}^{1/2}$

$$\theta(\Theta) = \tan^{-1} \frac{(y_2 - y_1) + \xi (y_3 - y_2)}{(x_2 - x_1) + \xi (x_3 - x_2)}$$

Interpolation functions N_i for the displacements u_i within the element are expressed as

$$N_1 = 1 + \rho \left(\frac{2 - 2^{(1-\lambda)}}{2^{(1-\lambda)} - 1} - \frac{\rho^{\lambda}}{2^{(1-\lambda)} - 1} \right)$$

$$N_2 = \rho (1-\xi) \frac{2^{(1-\lambda)}}{2^{(1-\lambda)} - 1} - \rho^{\lambda} \left[2\xi(1-\xi) + \frac{1-\xi}{2^{(1-\lambda)} - 1} \right]$$

$$N_3 = \rho\, \xi \frac{2^{(1-\lambda)}}{2^{(1-\lambda)} - 1} - \rho^{\lambda} \left[2\xi(1-\xi) + \frac{\xi}{2^{(1-\lambda)} - 1} \right] \tag{3.3}$$

$$N_4 = 2\rho \frac{1-\xi}{2^{(1-\lambda)} - 1} + 2\rho^{\lambda} \frac{1-\xi}{2^{(1-\lambda)} - 1}$$

$$N_5 = 4\rho^{\lambda} \xi (1-\xi)$$

$$N_6 = -\frac{2\rho\,\xi}{2^{(1-\lambda)} - 1} + 2\rho^{\lambda} \frac{\xi}{2^{(1-\lambda)} - 1}$$

The displacements $\underset{\sim}{u}^T = \{u,v,w\}$ can be decomposed into the following:

$$\underset{\sim}{u} = \sum_{i=1}^{6} \{ \rho^{\lambda}\ \underset{\sim}{N}_i^{(1)}(\xi) + \underset{\sim}{N}_i^{(2)}(\rho,\xi) \}\, \underset{\sim}{u}_i \tag{3.4}$$

Along $\theta = \theta_o$, i.e., the angle of the crack surface, the displacements are approximated by

$$\underset{\sim}{u} = \rho^{\lambda} \sum_{i=1}^{6} \underset{\sim}{N}_i^{(1)}(\xi_o)\, \underset{\sim}{u}_i \tag{3.5}$$

where $$\xi_o = \xi|_{\theta=\theta_o} = \frac{(x_2 - x_1)\tan\theta_o - (y_2 - y_1)}{(y_3 - y_2) - (x_3 - x_2)\tan\theta_o}$$

Thus the singular terms in the stress expression are

$$\underset{\sim}{\sigma} = r^{\lambda-1} \sum_{i=1}^{6} \underset{\sim}{Q_i}(\xi_o)\, \underset{\sim}{u_i} \tag{3.6}$$

where $\underset{\sim}{Q_i}$ is a matrix with elements related to the derivatives of shape functions and elastic constants.

3.2 Far-Field Element Formulation

Far-Field elements in the solid composite modeling are formulated based on generalized plane deformation theory and the minimum potential energy principle. Since no stress singularity is involved in the far field, formulation of the displacement-based element in a composite laminate under bending requires less effort than that given in the previous section for the construction of a singular element. A triangular element of the same nature has been proposed by Wang, et al[14] for a delamination problem in the composite laminate under in-plane stretching. To improve the rate of convergence of the solution, an eight-node isoparametric element is developed in this study in conjunction with the singular crack-tip element described in Sec. 3.1. A brief outline of derivations of the element stiffness and the associated loading vector of the far-field element is given here.

The potential energy functional Π_p to be minimized for the current element formulation in the absence of body force is given by :

$$\Pi_p = \iint_{A_m} \frac{1}{2} \underset{\sim}{\varepsilon}^T \underset{\sim}{C}\, \underset{\sim}{\varepsilon}\, dA - \iint_{s_{\sigma_m}} \underset{\sim}{T}^{*T}\, \underset{\sim}{u}\, ds \tag{3.7}$$

where $\underset{\sim}{\varepsilon}$ is a strain vector, $\underset{\sim}{C}$ is a 6x6 composite stiffness matrix, and $\underset{\sim}{T}^*$, the prescribed traction along s_{σ_m} of the mth element with an area A_m.

For the present problem of a composite laminate under bending M_x^∞, the displacement field may be written as

$$\underset{\sim}{u} = \underset{\sim}{u}_o + \underset{\sim}{U}(x,y) \tag{3.8}$$

where

$$\begin{aligned}
&\underset{\sim}{u}^T = \{u,v,w\},\\
&\underset{\sim}{u}_o{}^T = \{-1/2\, A_1 S_{33}\, z^2 - A_4 yz,\ -1/2\, A_2 S_{33} z^2 + A_4 xz,\ (A_1 x + A_2 y + A_3)\, S_{33} z\}\\
&\underset{\sim}{U}^T = \{\, U(x,y),\ V(x,y),\ W(x,y)\,\}
\end{aligned} \tag{3.9}$$

in which U(x,y),V(x,y) and W(x,y) are unknown functions to be determined.

Using an isoparametric element representation for U, V and W, one has

$$\underset{\sim}{U} = \underset{\sim}{N}\,\underset{\sim}{q} \tag{3.10}$$

where $\underset{\sim}{q}$ are nodal displacements and $\underset{\sim}{N}$ is a matrix of nodal interpolation functions. The modified strain-displacement relationship for the composite bending problem has the form,

$$\underset{\sim}{\varepsilon} = \underset{\sim}{\varepsilon}_o + \underset{\sim}{B}\,\underset{\sim}{q} \tag{3.11}$$

where $\underset{\sim}{\bar{\varepsilon}}^T = \{\varepsilon_x,\varepsilon_y,\gamma_{yz},\gamma_{xz},\gamma_{xy}\}$, $\underset{\sim}{\bar{\varepsilon}}_o^T = \{0,\ 0,\ (A_1 x + A_2 y + A_3) S_{33},\ A_4 x,\ -A_4 y,\ 0\}$, and $\underset{\sim}{B}$ is the differential form of $\underset{\sim}{N}$. Since $\underset{\sim}{N}$ is a function of x and y only, it is convenient to rewrite Eq. (3.11) in a simplified form as

$$\underset{\sim}{\bar{\varepsilon}}_{5x1} = \underset{\sim}{\bar{B}}_{5x24}\ \underset{\sim}{\bar{q}}_{24x1} \tag{3.12}$$

where $\underset{\sim}{\bar{\varepsilon}}^T = \{\, \varepsilon_x,\ \varepsilon_y,\ \gamma_{yz},\ \gamma_{xz},\ \gamma_{xy}\,\}$, and $\underset{\sim}{\bar{B}}$ is the reduced form of the aforementioned gradient matrix $\underset{\sim}{B}$.

The stress-strain relationship for a composite lamina under pure bending can be written in modified contracted notation:

$$\underset{\sim}{\bar{\sigma}} = \underset{\sim}{\bar{C}} \, (\underset{\sim}{\bar{\varepsilon}} - \underset{\sim}{\bar{\varepsilon}}_0) \tag{3.13}$$

where

$$\underset{\sim}{\bar{\sigma}}^T = \{ \sigma_x, \sigma_y, \tau_{yz}, \tau_{xz}, \tau_{xy} \}$$

$$\underset{\sim}{\bar{\varepsilon}}_0^T = \{ \varepsilon_{0i} \} = \{ S_{13}A_2y, S_{23}A_2y, -A_4x + S_{34}A_2y,$$

$$A_4y + S_{35}A_2y, S_{36}A_2y \},$$

$$\bar{C}_{5x5} = \{ \bar{S}_{5x5} \}^{-1} \qquad (i,j=1,2,4,5,6)$$

and $\bar{S}_{ij}$ is the reduced compliance tensor of each lamina. The stress component, $\sigma_z=\sigma_3$, is obtained from

$$\sigma_3 = A_1x + A_2y + A_3 - S_{3j}\,\sigma_j/S_{33} \tag{3.14}$$

In terms of $\underset{\sim}{\bar{\varepsilon}}$ and $\underset{\sim}{\bar{\varepsilon}}_0$, the potential energy functional, Π_p, at an element level can be written as follows:

$$\Pi_p = \iint_{A_m} \frac{1}{2} \underset{\sim}{\bar{\varepsilon}}^T \underset{\sim}{\bar{C}} \underset{\sim}{\bar{\varepsilon}} \, dA - \iint_{A_m} \frac{1}{2} \underset{\sim}{\bar{\varepsilon}}^T \underset{\sim}{\bar{C}} \underset{\sim}{\bar{\varepsilon}}_o \, dA + \frac{1}{2} \iint_{A_m} \underset{\sim}{\bar{\varepsilon}}_o^T \underset{\sim}{\bar{C}} \underset{\sim}{\bar{\varepsilon}}_o \, dA$$

$$- \int_{s_{\sigma_m}} \underset{\sim}{T}^{*T} \underset{\sim}{u} \, ds + C_o \tag{3.15}$$

where C_o is a constant related to $\underset{\sim}{\varepsilon}_o$.

Following the standard variational procedure of minimum potential energy, one can obtain the element stiffness $\underset{\sim}{k}$ and the consistent loading vector $\underset{\sim}{Q}$ as

$$\underset{\sim}{k} = \iint_{A_m} \underset{\sim}{\bar{B}}^T \underset{\sim}{\bar{C}} \underset{\sim}{\bar{B}} \, dA \tag{3.16}$$

$$\underset{\sim}{Q} = \iint_{A_m} \underset{\sim}{\bar{B}}^T \underset{\sim}{\bar{C}} \underset{\sim}{\bar{\varepsilon}}_o \, dA + \int_{s_{\sigma_m}} \underset{\sim}{N}^T \underset{\sim}{T}^* \, ds \tag{3.17}$$

for a far-field element in the modeling of the bending problem of a delaminated composite laminate.

3.3 Solution Scheme and Algorithm

Based on a displacement-based finite element method, it is convenient to apply extensional, bending and torsional deformations, i.e., A_1, A_2, A_3, and A_4,in the formulation. It is well known that, in general, bending of a composite laminate is accompanied by extension and torsion. Based on the superposition principle of linear elasticity, total deformation under mechanical loading can be expressed as a linear combination of the extentional, bending, and torsional deformations. Written in the mathematical form, one has

$$\begin{bmatrix} A_1 S_{33} \\ A_2 S_{33} \\ A_1 S_{33} \\ A_4 \end{bmatrix} = \begin{bmatrix} D_{11} & D_{12} & D_{13} & D_{14} \\ D_{12} & D_{22} & D_{23} & D_{24} \\ D_{13} & D_{23} & D_{33} & D_{34} \\ D_{14} & D_{24} & D_{34} & D_{44} \end{bmatrix} \begin{bmatrix} M_y^\infty \\ M_x^\infty \\ M_z^\infty \\ M_t^\infty \end{bmatrix} \tag{3.18}$$

where $M_y^\infty = M_t^\infty = 0$ and $F_z^\infty = 0$ in the present case. The symmetry of the $\underset{\sim}{D}$ matrix is assured by Betti's reciprocal theorem.

By inverting the above equation, the induced extensional, bending and torsional deformations under applied bending are obtainable.

4. Delamination Stress Intensity Factors and Energy Release Rates

Fracture mechanics parameters, such as crack-tip stress intensity factors and energy release rates for a delamination, are evaluated from the asymptotic solutions for interlaminar stresses σ_2,σ_6 and σ_4(or σ_y, τ_{xy}, and τ_{yz}) and the displacements u_i along the plane of the crack. For a finite-dimensional composite laminate containing a delamination, the asymptotic stress and displacement fields can be conveniently determined by the aforementioned singular finite-element method. Along the delamination plane $\xi = \xi_o$, the near-field stresses and displacements are approximated by using Eq. (3.7) and its derivatives as

$$\underset{\sim}{\sigma} \simeq \rho^{\delta}\ \underset{\sim}{R}(\xi_o;\delta)\ \underset{\sim}{q} \tag{4.1a}$$

$$\underset{\sim}{u} \simeq \rho^{\delta+1}\ \underset{\sim}{M}(\xi_o)\ \underset{\sim}{q} + \underset{\sim}{u}_o, \tag{4.1b}$$

where $\underset{\sim}{R}(\xi_o;\delta)$ is a matrix of derivatives of the shape functions $\underset{\sim}{M}$ and ply elastic constants. The ρ and ξ_o are related to the global coordinates by a simple transformation given in [14].

For a partially closed delamination or a delamination with a very small size of crack-tip closure for which the simplified model [11] with an inverse square-root stress singularity is used, the stress intensity factors and strain energy release rates can be evaluated easily. Taking $\underset{\sim}{\sigma}$ and $\underset{\sim}{u}$ along the crack plane $\xi_o = 0$ (i.e., $\phi_o = 0$), the asymptotic interlaminar stress and displacement along the ply interface can be written in a form as

$$\sigma_i \simeq A_k\, r^{-1/2} \qquad (i=2,\ k=1;\ i=6,\ k=2,\ \text{and}\ i=4,\ k=3), \tag{4.2a}$$

$$u_j \simeq B_k\, r^{1/2} + u_{oj} \qquad (j=1,\ k=2;\ j=2,\ k=1,\ \text{and}\ j=3,\ k=3), \tag{4.2b}$$

where A_k and B_k are obtained from the corresponding components of $\underset{\sim}{R}(\xi_o;\delta)$ and $\underset{\sim}{M}(\xi_o)$ in Eqs. (4.1(a)) and ((4.1(b)) by setting $\xi_o = 0$ and $\delta = -1/2$. Thus, the delamination stress intensity factors K_i can be easily determined by

$$K_i = \sqrt{2\pi}\ A_i \qquad (i=I,II,III). \tag{4.3}$$

The energy release rates can be determined in a manner similar to that for K_i as:

$$G = G_1 + G_2 + G_3$$

$$= \lim_{\delta a \to 0} \frac{1}{2\delta a} \int_0^{\delta a} \{ \sum_{k=1}^{3} (A_k r^{-1/2}) [B_k (\delta a - r)^{1/2}] \} dr$$

$$= \lim_{\delta a \to 0} \frac{1}{2\delta a} \int_0^{\delta \alpha} \sum_{k=1}^{3} A_k B_k \left(\frac{\delta a - r}{r} \right)^{1/2} dr \qquad (4.4)$$

The term u_{oj} in Eq. (4.2b) is not included, because it does not result in any contributions to G_i and G after integration. Integration of the singular integral Eq. (4.4) can be carried out explicitly. The strain energy release rates have the form

$$G = \sum_{k=1}^{3} G_i = \frac{\pi}{4} (A_1 B_1 + A_2 B_2 + A_3 B_3). \qquad (4.5)$$

We remark here that each term in Eq. (4.5) corresponds to an individual G_i and that for a delamination with a finite length of crack closure, the first term in Eq. (4.5) is identically zero, i.e., $G_1 = 0$.

5. Results and Discussion

The aforementioned analytical and numerical methods have been applied to a delamination problem in a fiber-reinforced composite laminate subjected to bending to illustrate solution convergence and computational efficiency. A schematic finite element discretization for a half of the composite laminate cross section is shown in Fig. 2. A six-node singular element with eighteen degrees of freedom (3 DOF per node) around the crack tip, shown in Fig. 3, is constructed in conjunction with the eight-node, quasi three-dimensional, nonsingular element in the surrounding region. Compatibility between the two kinds of elements is ensured in their formulations (Secs. 3.1 and 3.2). The non-singular finite elements are refined near the crack tip region to take care of the high stress gradient. The influence of the size of the singluar element on convergence and efficiency of the present approach is demonstrated in this section.

For illustrative purposes, numerical results for a $[45/-45]_s$ graphite-epoxy composite with two edge delaminations under bending is considered. (The fiber orientation θ is defined as the angle between the fibers and the z-axis.) The composite has a geometry of b = 2 in., h = 0.25 in. and a/b = 0.35. Due to the out-of-plane loading mode and the geometric symmetry, only one half of the cross section is needed. Assume that each lamina is made of graphite-epoxy with the following elastic properties:

$$E_L = 19.5\ 10^6 \text{ (psi)}, \qquad E_T = E_Z = 1.48\ 10^6 \text{ (psi)},$$
$$G_{LT} = G_{LZ} = 0.8\ 10^6 \text{ (psi)}, \qquad G_{TZ} = 0.49\ 48\ 10^6 \text{ (psi)},$$
$$\upsilon_{LT} = \upsilon_{LZ} = 0.3, \qquad \upsilon_{TZ} = 0.49.$$

where L, T, and Z refer to the principal material axes along fiber, transverse, and thickness directions, respectively.

For symmetric angle ply composites under pure bending, symmetry conditions for displacements with respect to the y-z plane lead to the following relationships:

$$\begin{aligned} U(x,y) &= U(-x,y) \\ V(x,y) &= V(-x,y) \\ W(x,y) &= W(-x,y) \end{aligned} \tag{5.1}$$

5.1 Size Effect of the Singular Element

In the analysis of a delaminated composite laminate, the singular elements are required to cover a finite region at the crack tip so that the deformation in the singular-stress domain can be accurately determined. It is recognized that the singular domain is small in general and that the shape functions consist of only dominant singular terms and the terms for the nonsingular field. Thus sizes of the crack-tip elements are of significant importance in the solution accuracy and efficiency of numerical results. In this study, a total of twelve equal-size elements around the crack tip, shown in Fig. 3, are used to cover the singular domain. The size effect of the singular element on solution convergence and efficiency may be characterized by a non-dimensional parameter η, defined as

$$\eta = \frac{\Delta a}{h} = \frac{\text{linear dimension of the singular element}}{\text{lamina thickness}}$$

In Fig. 4, the normalized stress intensity factors K_i (i = I, II, III) in the delaminated composite change as the size parameter η reduces from 0.01 to 0.001. In all of the cases, the variations are less than 3 percent in the acceptable range. It indicates that the present solutions are converged and stable. Thus, in all of the later analysis, $\eta = 0.004$ is used.

5.2 Effect of Number of Elements around the Crack Tip

In the singular element formulation, shape functions for the dominant singular, nonsingular terms (eq. 3.4) are quadratic and linear in θ, respectively. The minimum number of singular element enclosing the tip region, which would provide sufficient angular variations in the near field, is an important computational parameter to be determined for the solution convergence and efficiency. The $2\pi/n$ is the size parameter for the solution convergency and accuracy. This effect may be clearified by examining the resulting stress field near the crack tip and the stress intensity factors. The results are given in Fig. 5. As the elements increase from eight to 20, the K_i (i = I,

II, III) alter only by less than 4%, 1%, and 1%, respectively. Thus, the use of a proper number of the singular element around the crack tip ensures the solution accuracy and convergency, if n > 8.

5.3 Effect of Lamina Thickness and Delamination Location

An important issue investigated in this study is the effect of laminate thickness, since transverse deformation and failure are affected significantly by lateral/transverse constraints in a composite laminate. In this paper, a delaminated $[45/-45]_S$ graphite-epoxy laminate with various b/h's are considered with b being kept constant. For an edge-delamination case, as shown in Fig. 6, the results indicate that, for a composite with given laminate configuration, the change in ply thickness b/h does not alter the values of K_i significantly. The high value of K_{III} relative to K_I indicate that mode-III crack growth and fracture may be the dominant failure mode. However, in a case of a delamination with short length, interaction of the free edge with the delamination becomes crucial. In the case of a center delamination in the composite laminate as shown in Fig. 7, it is found that the delamination crack growth becomes more dominated by mode I deformation as the ply thickness increases. The high value of K_I introduced by the increase in laminate thickness provides a clear basis for evaluation of failure mechanisms in thick-section composite laminates.

5.4 Effect of Crack Length

Fracture of a composite laminate resulting from delamination crack growth, is often observed in the experiment. Failure processes may experience stable, unstable crack growth or a combination of these. Thus, the effect of crack length on interlaminar crack-tip stresses may provide a rational basis of understanding the delamination growth behavior. The rapid increase in K_i and G_i for the center delamination cases in a graphite-epoxy composite is shown in Figs. 8-14. In contrast to the uniform stretching case, fracture of a delaminated composite subjected to bending may be catastropic, as all of the K_i and G_i increases monotonically as the value of a/b increases rapidly.

5.5 Effect of Laminate Layup

Figures 15-21 illustrate the significant effect of fiber orientation on the crack-tip interlaminar stresses in $[\theta/\theta]_S$ graphite/epoxy thick composite laminates with various delamination lengths. For a center delamination case, the value of K_I varies appreciably with as depicted in Fig. 15. The K_I value reaches a plateau as θ approaches 45°. As the crack length increases, a larger K_I is observed. A similar trend is shown in Fig. 16 for K_{II}. Opposite tendency of the crack length effect is noticed. The important fracture mechanics parameter, K_{III} versus θ, is shown in Fig. 17. The value of K_{III} increases first and then decreases with the ply angle θ. Note that θ = 37.5° is observed to introduce the maximum K_{III} for all of the crack lengths studied. For an edge delamination case, a similar behavior to the center delamination case is observed for the K_{III}. However, the longer the delamination, the larger the K_{III}. A similar behavior is given in Figs. 18-21 in which G_I, G_{II} and G_{III} as a function of ply angle θ are shown.

6. Conclusions

In this study, both a crack-tip asymptotic analysis and advanced numerical methods have been introduced to solve the delamination crack problem in a fiber composite laminate subjected to out-of-plane bending. The structure of the near-field solution has been determined by an eigenfunction expansion method. The full-field solution is determined by a conformal-mapping singular finite element analysis, based on the mathematical structure of the elasticity solution, numerical results are obtained for various cases with different lamination and crack parameters in the composite bending problem. Based on the methods developed and the results obtained, the following conclusions may be reached:

1. The crack-tip asymptotic solution for a delaminated composite laminate under bending can be determined by an eigenfunction expansion method.
2. A near-field singular element can be constructed on the basis of the asymptotic solution obtained and the conformal mapping method introduced by Stern [13].
3. In conjunction with the near-field singular element, a nonsingular composite bending element is also constructed based on the composite laminate elasticity solution for bending.
4. The numerical methods developed lead to both the local crack-tip solution and and the far-field deformation and stress in a delaminated composite under out-of-plane bending.
5. The effect of composite laminar thickness is found to be very significant on the delamination crack-tip stress intensities and associated energy release rates for a composite containing an interior delamination under external bending. However, much less appreciable influence is observed for a delamination located at the edge of the composite under nominal bending.
6. The increase in laminar thickness may alter the failure mode of an interior delamination

under bending. Failure modes change from shear modes to the opening mode in a composite laminate subjected to out-of-plane bending. However, no appreciable change in the failure mode is found for an edge delamination case.

7. In an angle-ply $[\theta/-\theta]_S$ composite laminate containing a delamination in the upper interface, the fiber orientation θ has very significant effects on the delamination crack-tip stress intensities and energy release rates.

8. Significant delamination surface closure is found in composite specimens with both an edge delamination and a center interior delamination at the upper interface in the composite laminate under bending for the cases of $\theta \leq 7.5°$. Shear failure, thus, dominates the composite delamination crack growth behavior.

7. Acknowledgements

The research work described in this paper was supported in part by National Aeronautics and Space Administration-Langley Research Center (NASA-LaRC), Hampton, VA under Grant NAG 1-286. The authors are grateful to Drs. T. K. O'Brien and N. Johnston of NASA-LaRC for their support and fruitful discussion.

8. References

1. S. S. Wang, "An Analysis of Delamination in Angle-ply Fiber Reinforced Composites", ASME Journal of Applied Mechanics, Vol. 17, 1980, pp. 64-70.

2. J. D. Whitcomb, "Finite Element Analysis of Instability Related Delamination Growth", Journal of Composite Materials, Vol. 15, pp. 403-426.

3. K. T. O'Brien, "Characterization of Delamination Onset and Growth in a Composite Laminates", Damage in Composite Materials, ASTM STP 775, K. L. Reifsnider, Ed., American Society for Testing and Materials, Philadelphia, PA, 1982, pp. 140-167.

4. K. S. Kim and C. S. Hong, "Delamination Growth in Angle-Ply Laminated Composites", Journal of Composite Materials, Vol. 20, 1986, pp. 423-438.

5. G. A. Kardomateus and D. W. Schmuser, "Buckling and Postbuckling of Delaminated Composites under Compressive Loading", AIAA Journal, Vol. 27, 1989, pp. 624-631.

6. N. J. Pagano, "Exact Solutions for Composite Laminates in Cylindrical Bending", Journal of Composite Materials, Vol. 3, 1969, pp. 398-411.

7. K. W. Chan and O. O. Ochoa, "An Integrated F. E. model for Edge Delamination Analysis of Laminates due to Tension, Bending and Torsional Loads", Proceedings of AIAA/ASME/ASCE/AHS Structures, Structural Dynamics and Materials Conference, 1987; also, appear in Journal of Computational Mechanics.

8. S. G. Lekhnitskii, "Theory of Elasiticity of an Anistropic Elastic Body", Holden-Day, Inc., San Francisco, CA, 1963.

9. S. S. Wang, "Elasticity Solutions for a Class of Composite Laminate Problems with Stress Singularities", Mechanics of Composite Materials, (Proceedings of IUTAM Symposium on Mechanics of Composite Materials), Z. Hashin and C. T. Herakovich, Eds., Pergamon Press, New York, 1983, pp. 259-281.

10. S. S. Wang and I. Choi, "Mechanics of Delamination in Fiber-Reinforced Composite Materials, Part I: Stress Singularities and Solution Structures", Mechanics of Composite Materials, AMD - Vol. 58, American Society of Mechanical Engineers, New York, 1983, pp. 83-104.

11. S. S. Wang and I. Choi, "The Interface Crack Between Dissimilar Anistropic Composite Materials", ASME Journal of Applied Mechanics, Vol. 50, 1983, pp. 169-178.

12. S. S. Wang and I. Choi, "Interface Crack Behavior in Dissimilar Anistropic Composite under Mixed Mode Loading", ASME Journal of Applied Mechanics, Vol. 50, 1983, pp. 179-183.

13. M. Stern, "Families of Consistent Conforming Elements with Singular Derivative Fields", International Journal for Numerical Methods in Engineering, Vol. 14, 1979, pp. 409-421.

14. S. S. Wang and I. Choi, "Mechanics of Delamination in Fiber-Reinforced Composite Materials, Part II: The Delamination Behavior and Fracture Mechanics Parameters", Mechanics of Composite Materials, AMD - Vol. 58, American Society of Mechanical Engineers, New York, 1983, pp. 105-134.

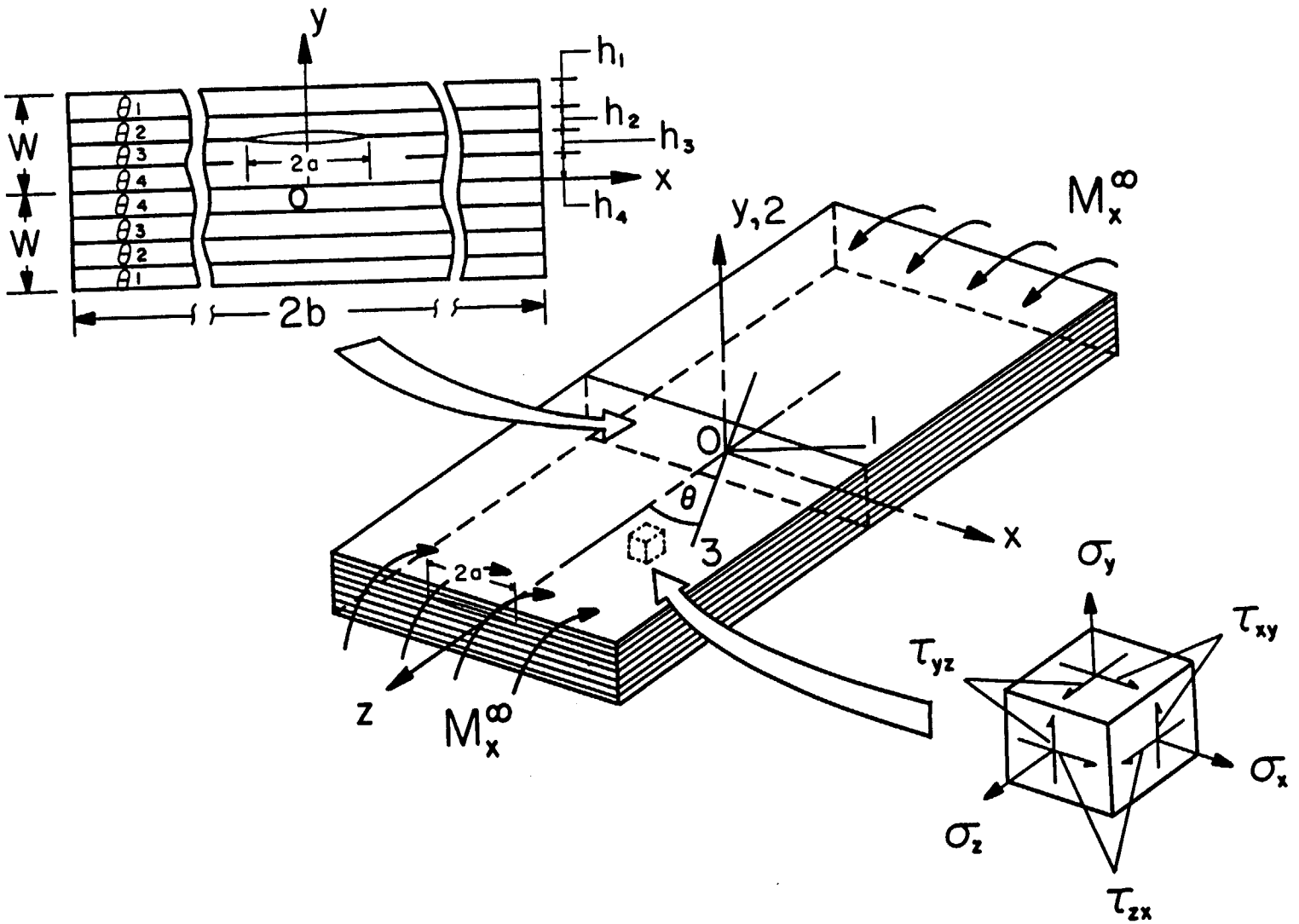
y
h1
h2
h3
h4
x
θ1
θ2
θ3
θ4
θ4
θ3
θ2
θ1
W
W
2a
O
2b
y,2
M∞x
O
1
θ
x
3
2a
z
M∞x
σy
τxy
τyz
σx
σz
τzx

Fig. 1

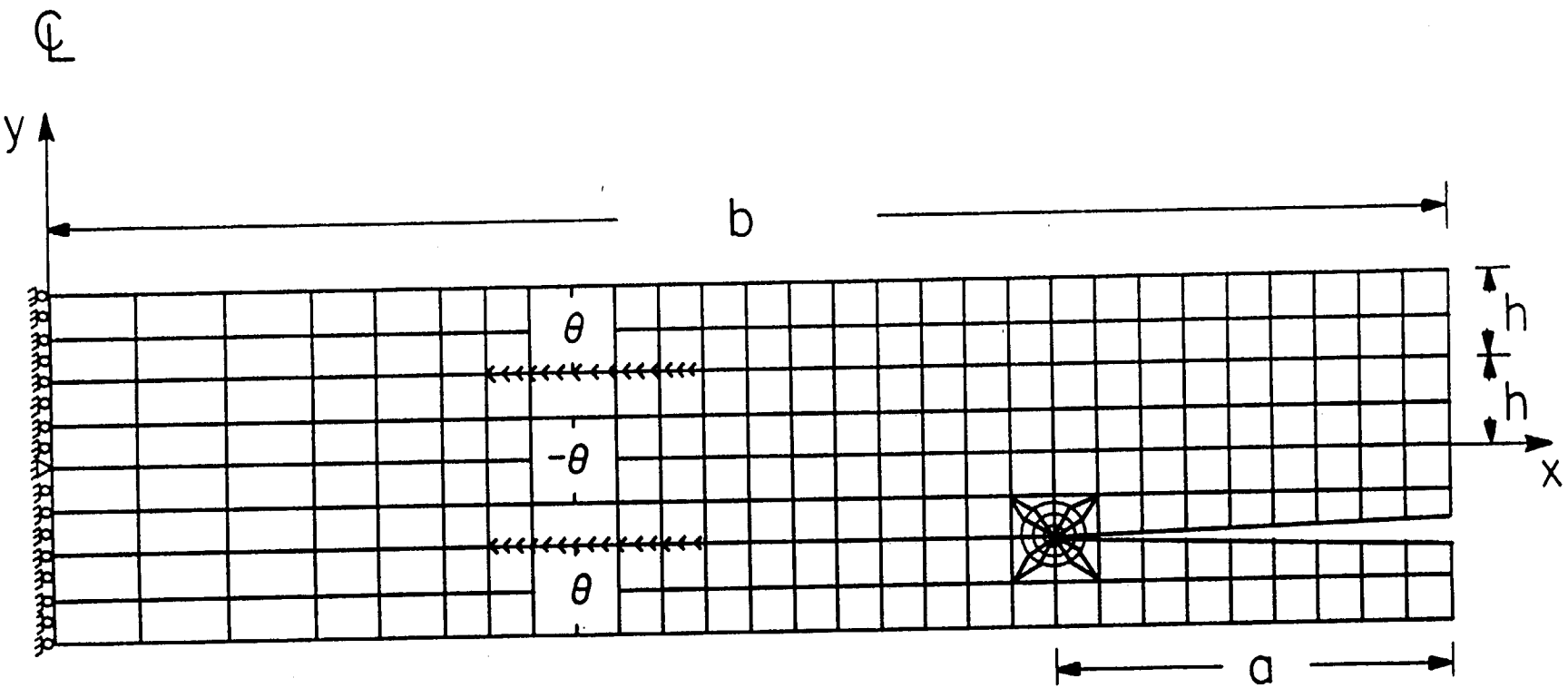

Fig. 2

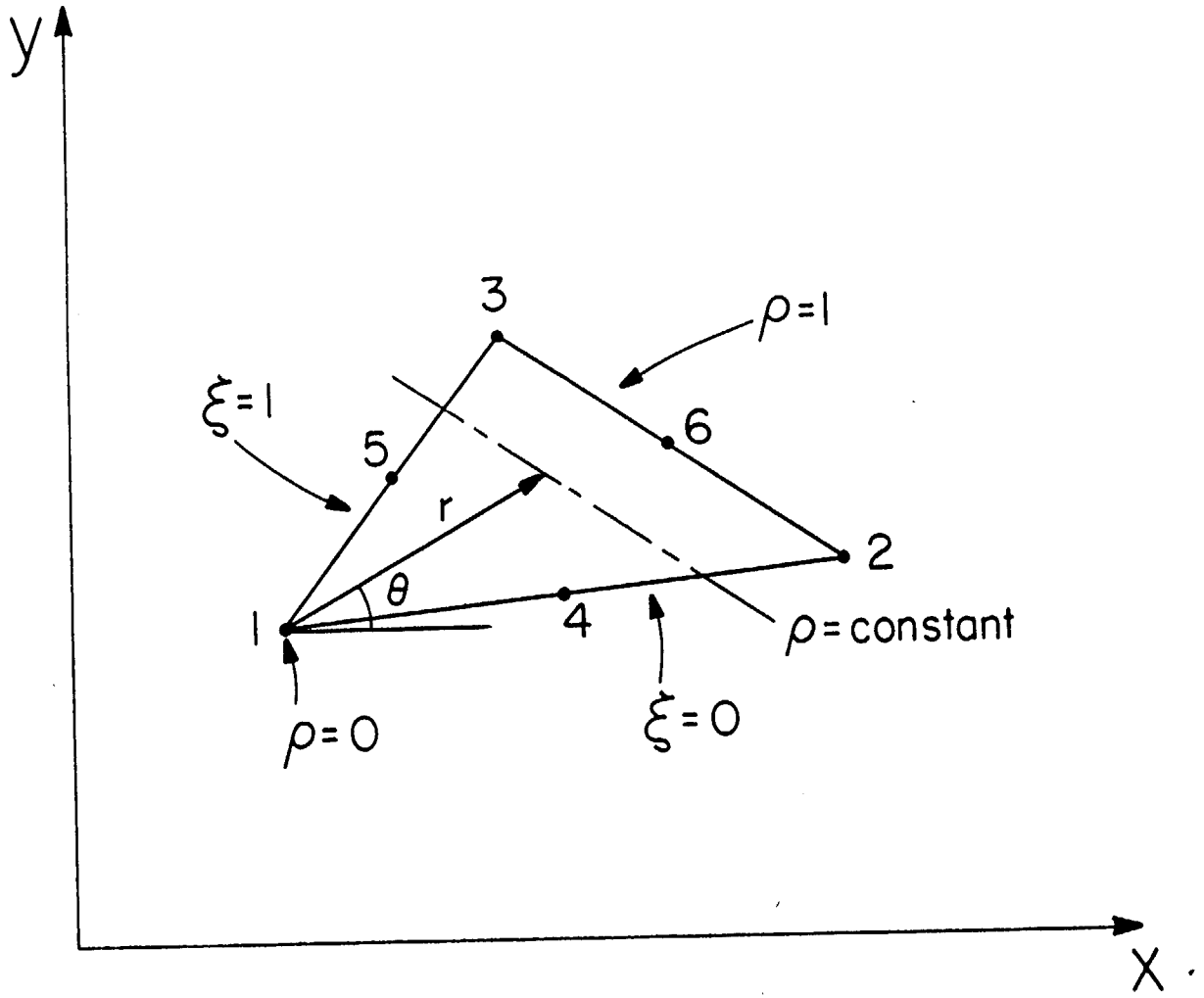

Fig. 3

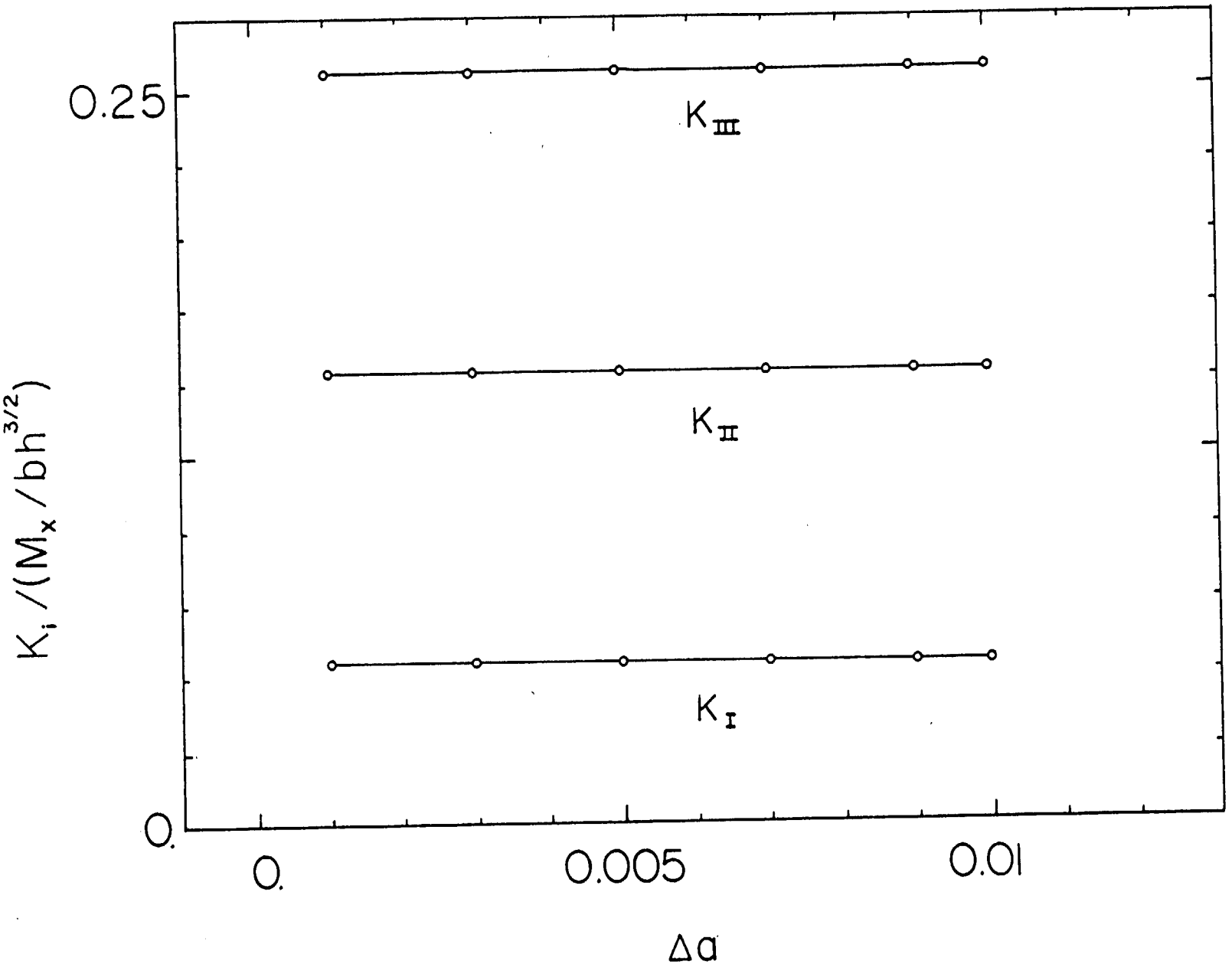

Fig. 4

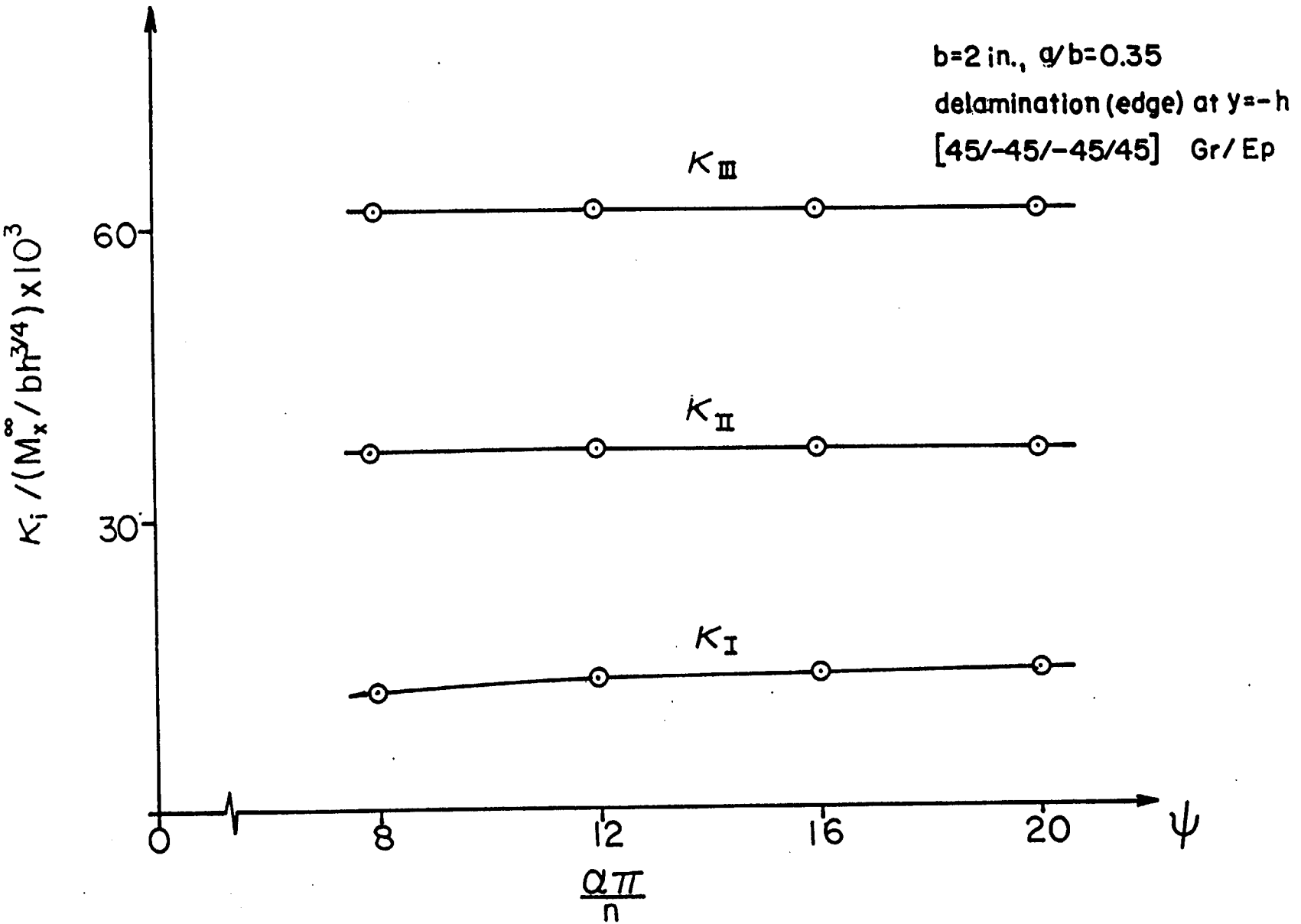
b=2 in., a/b=0.35
delamination (edge) at y=-h
[45/-45/-45/45] Gr/Ep
K_{III}
K_{II}
K_I
$K_i/(M_x^\infty/bh^{3/4})\times10^3$
60
30
0
8
12
16
20
ψ
$\frac{\alpha\pi}{n}$

Fig. 5

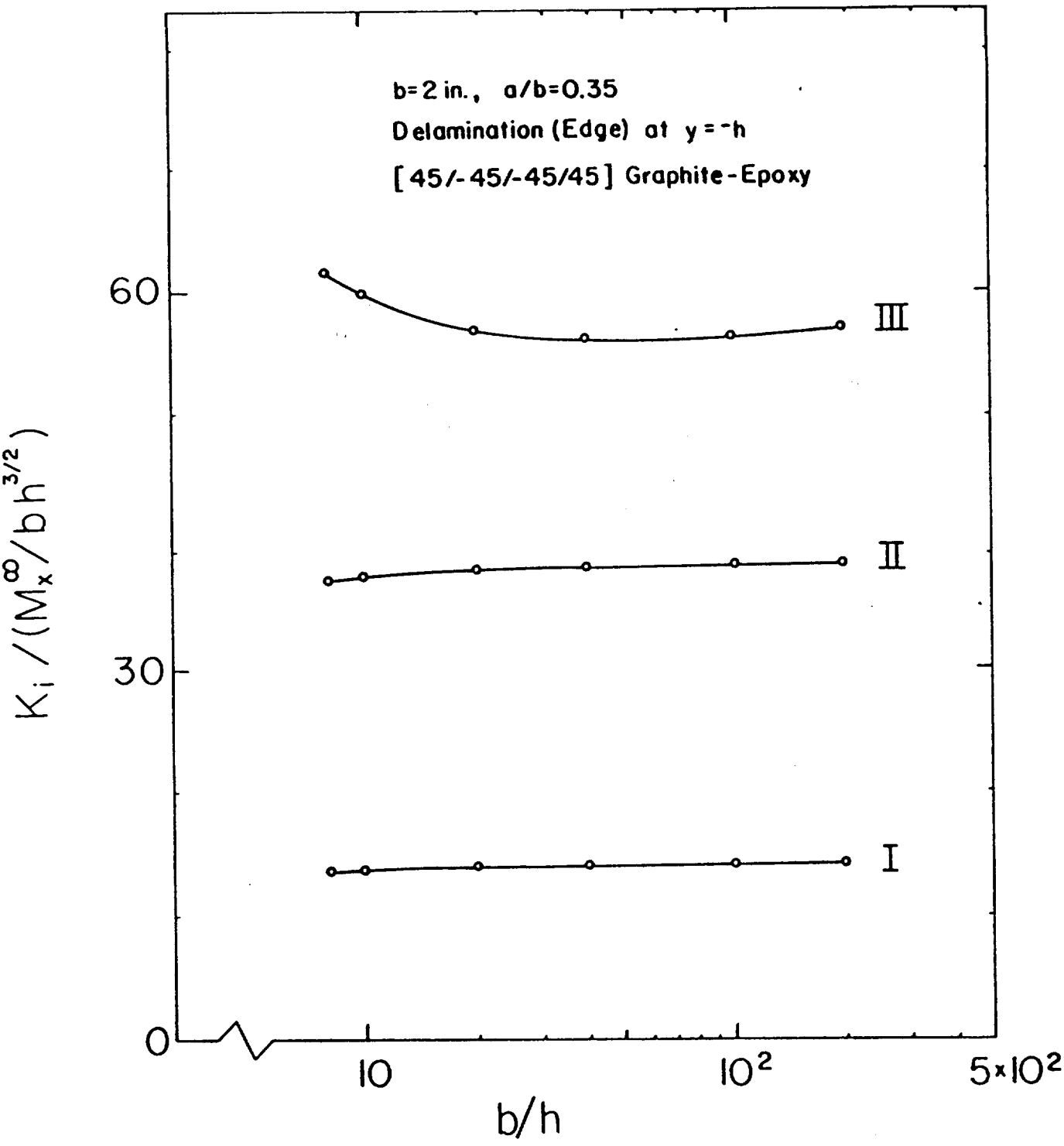

Fig. 6 Effect of laminate thickness on stress intensity factors

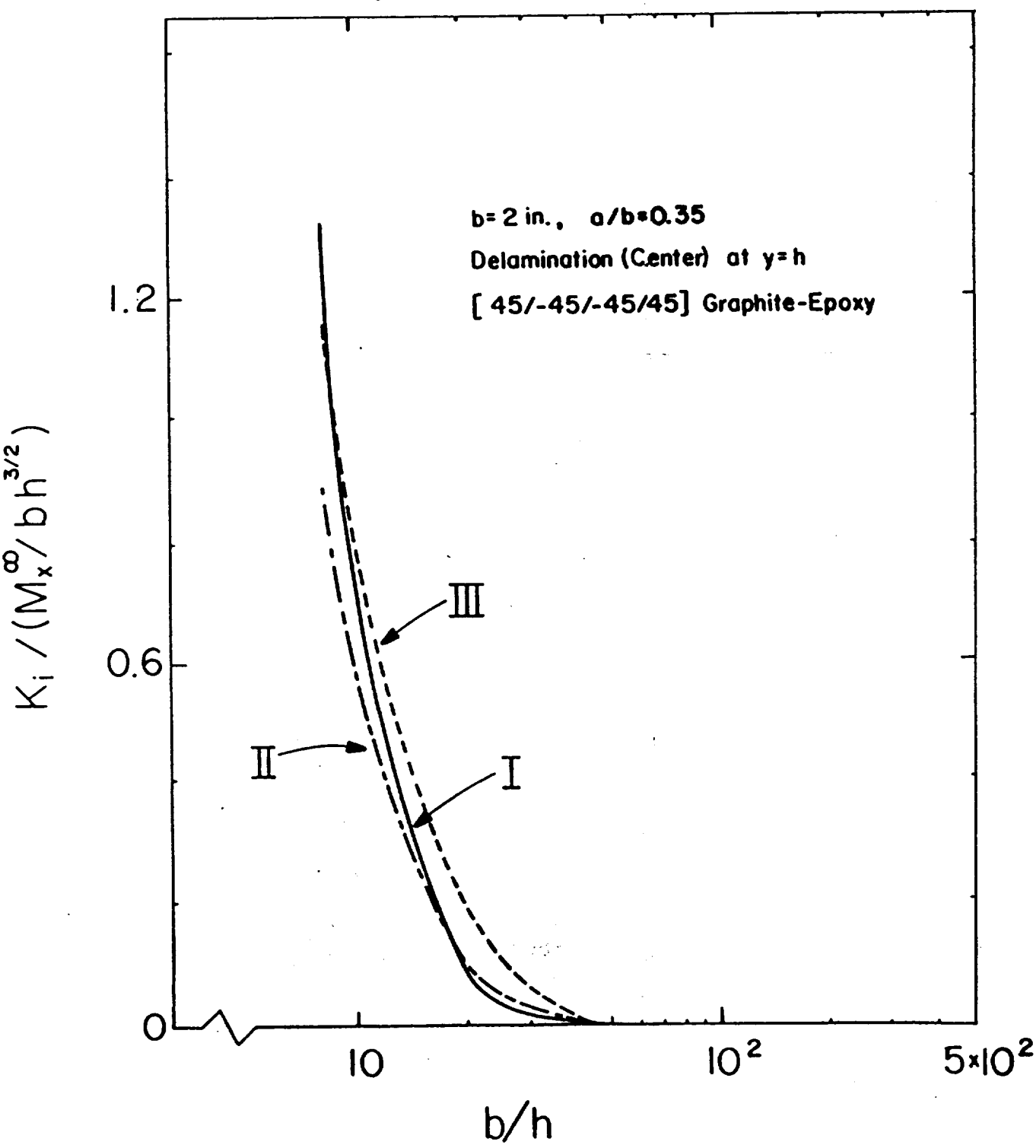

Fig. 7 Effect of laminate thickness on stress intensity factors

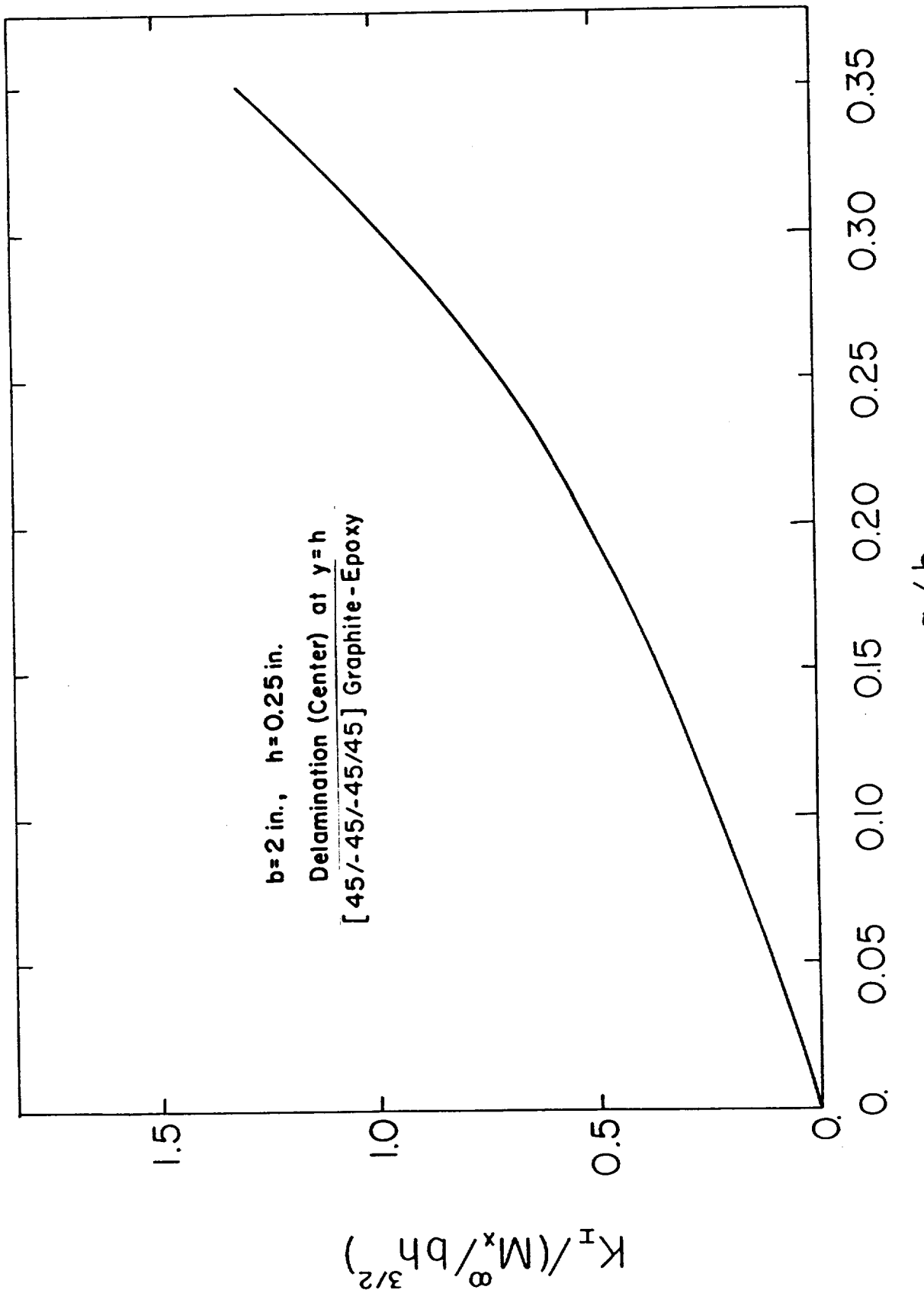
b=2 in., h=0.25 in.
Delamination (Center) at y=h
[45/-45/-45/45] Graphite-Epoxy
$K_I/(M_x^0/bh^{3/2})$
a/b
0.
0.05
0.10
0.15
0.20
0.25
0.30
0.35
0.5
1.0
1.5

Fig. 8

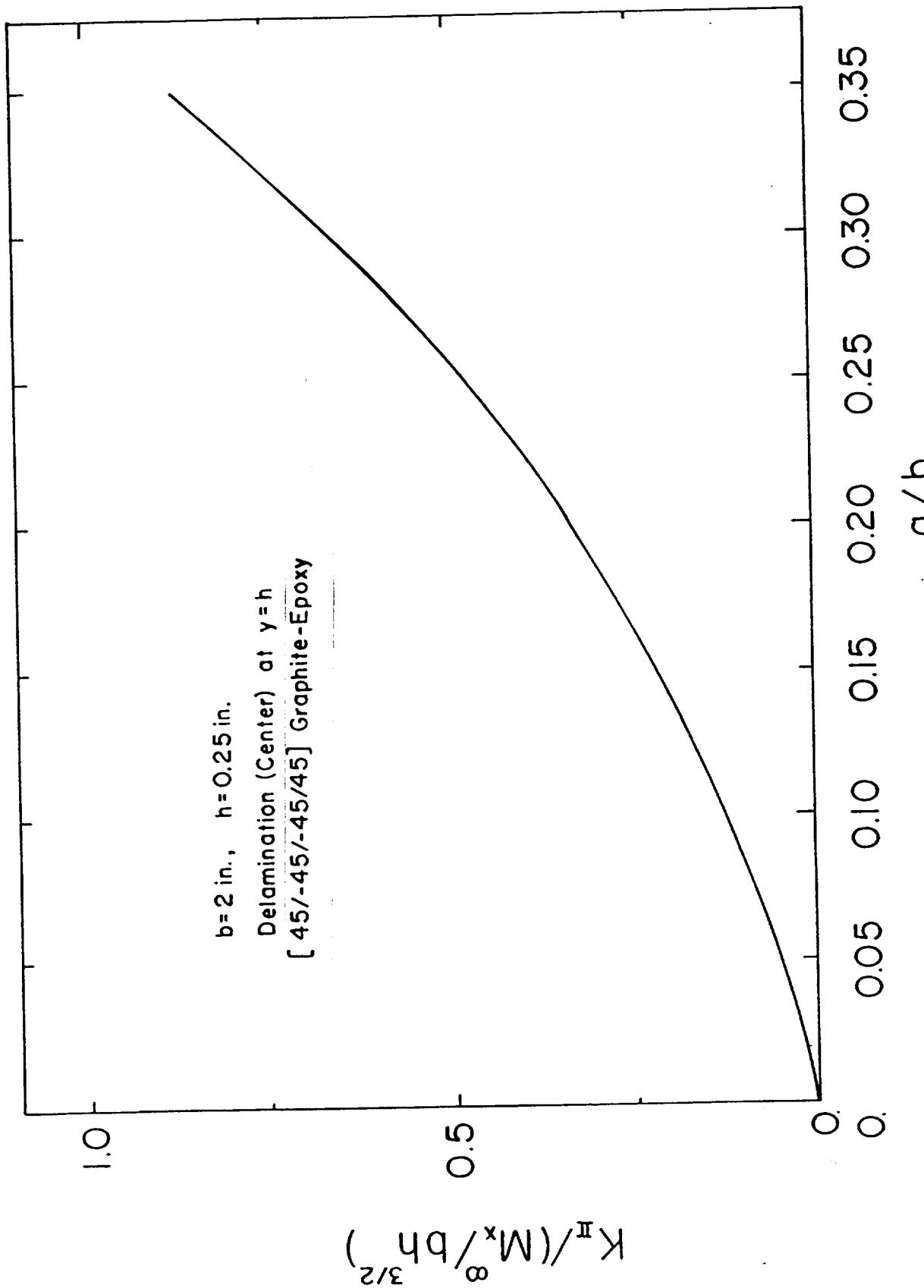
b=2 in., h=0.25 in.
Delamination (Center) at y=h
[45/-45/-45/45] Graphite-Epoxy
$K_{II}/(M_x^0/bh^{3/2})$
a/b
0.
0.5
1.0
0.05
0.10
0.15
0.20
0.25
0.30
0.35

Fig. 9

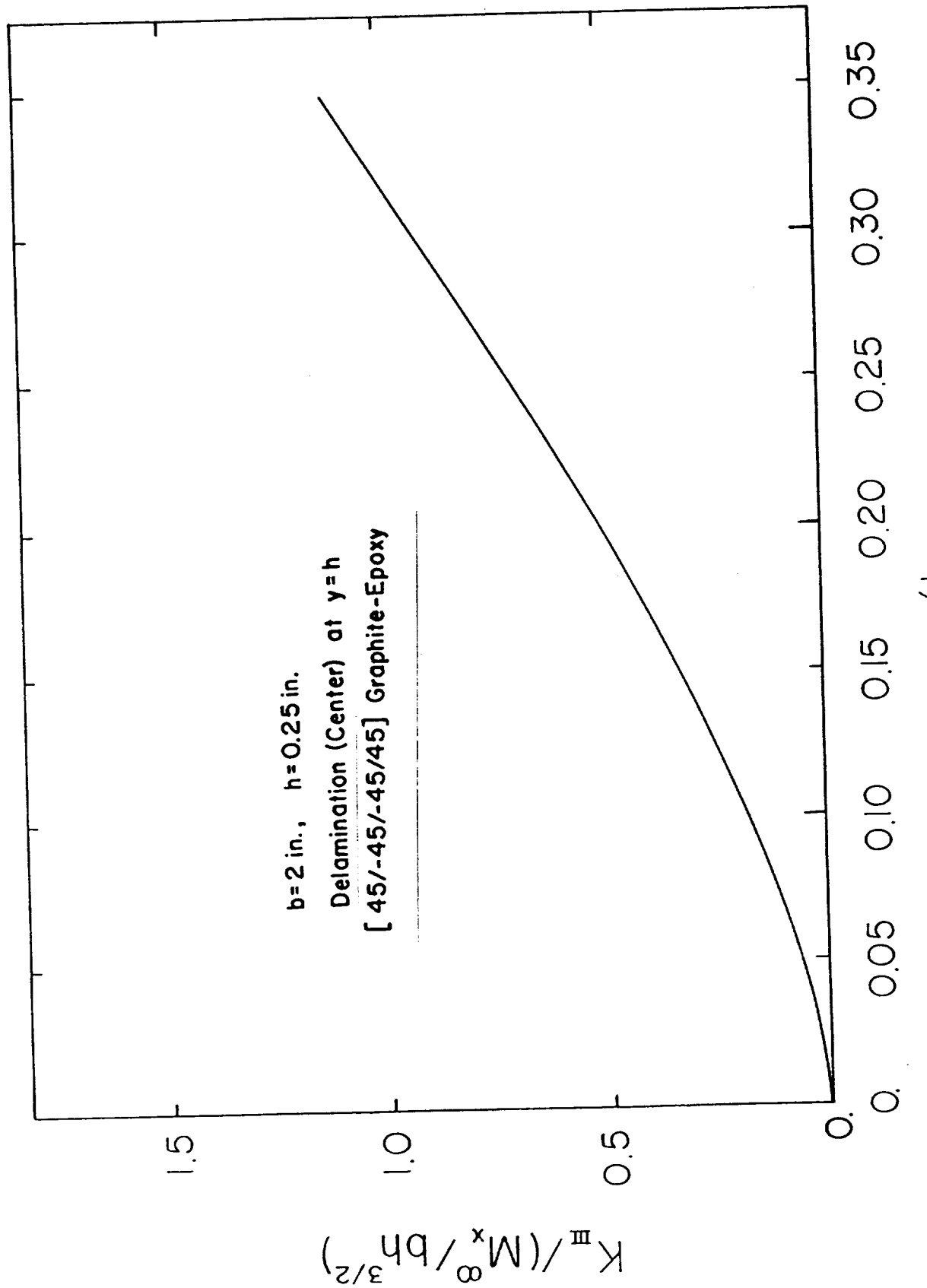
b=2 in., h=0.25 in.
Delamination (Center) at y=h
[45/-45/-45/45] Graphite-Epoxy
$K_{III}/(M_x^0/bh^{3/2})$
a/b
0.
0.05
0.10
0.15
0.20
0.25
0.30
0.35
0.5
1.0
1.5

Fig. 10

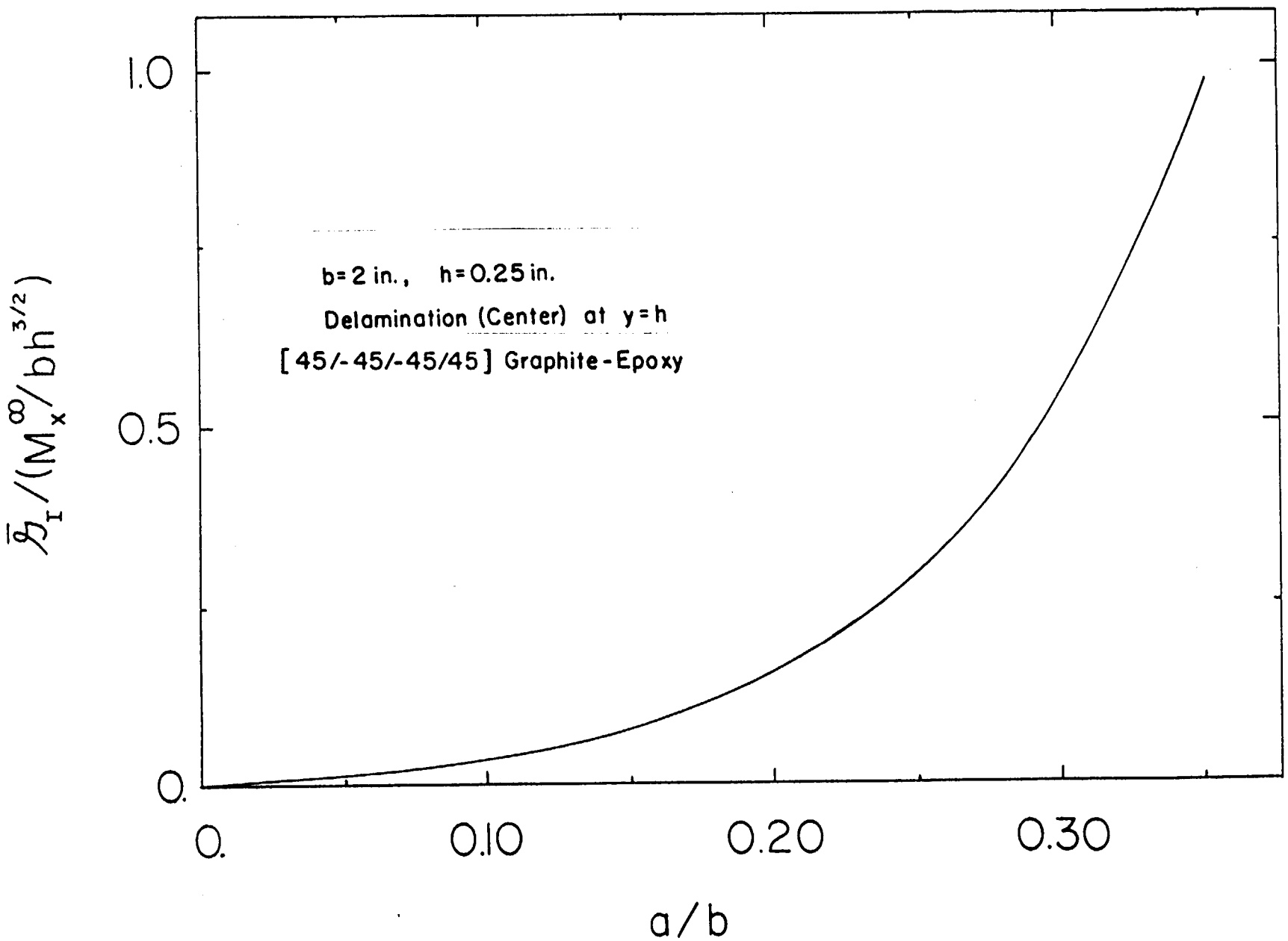
1.0
0.5
0.
0.
0.10
0.20
0.30
a/b
$\bar{\mathcal{G}}_I/(M_x^\infty/bh^{3/2})$
b=2 in., h=0.25 in.
Delamination (Center) at y=h
[45/-45/-45/45] Graphite-Epoxy

Fig. 11

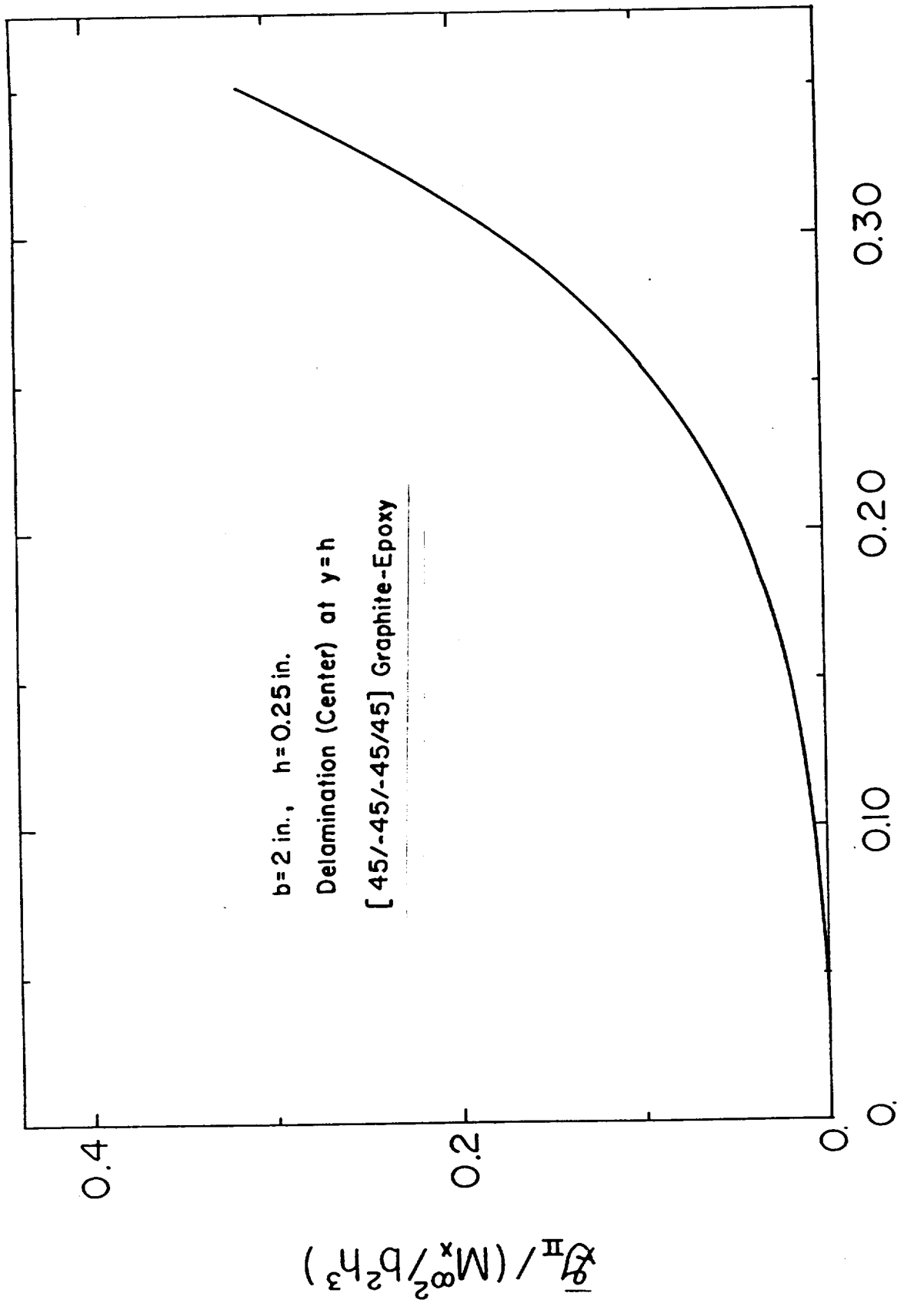
$\bar{\psi}_{II}/(M_x^{\infty 2}/b^2h^3)$
0.4
0.2
0.
0.
0.10
0.20
0.30
a/b
b=2 in., h=0.25 in.
Delamination (Center) at y=h
[45/-45/-45/45] Graphite-Epoxy

Fig. 12

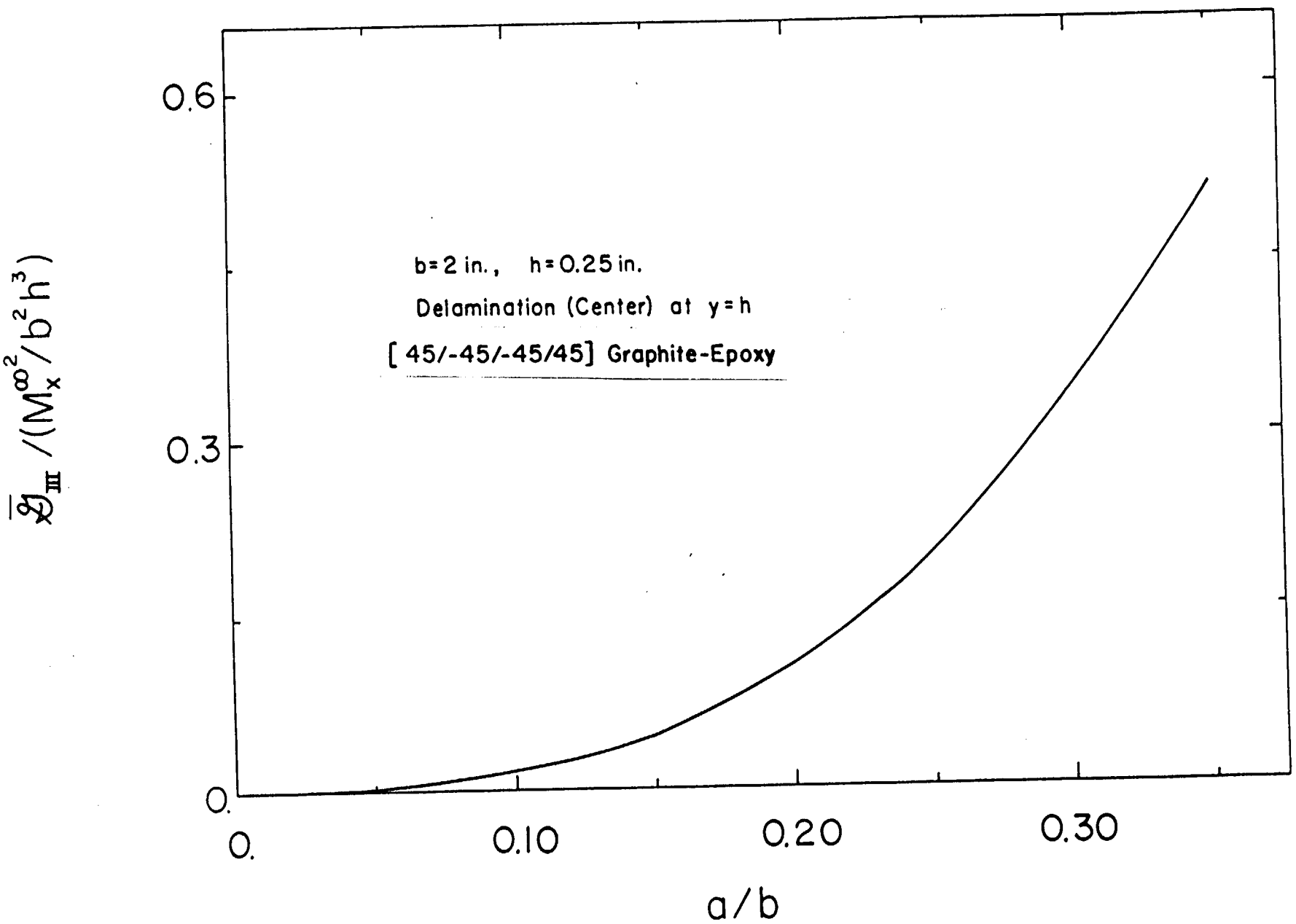
$\bar{\mathcal{G}}_{III}/(M_x^{\infty 2}/b^2h^3)$
0.6
0.3
0.
0.
0.10
0.20
0.30
a/b
b=2 in., h=0.25 in.
Delamination (Center) at y=h
[45/-45/-45/45] Graphite-Epoxy

Fig. 13

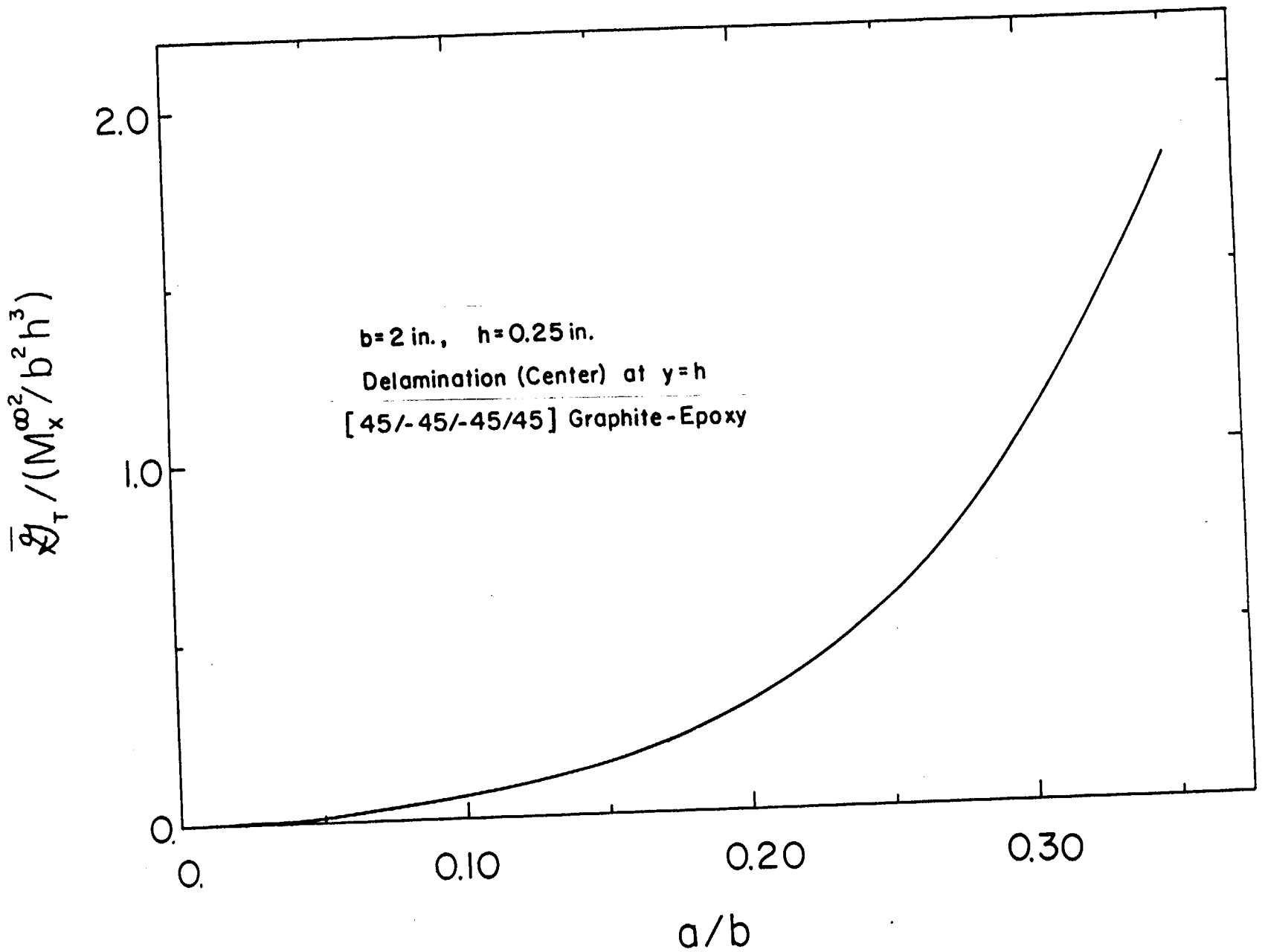
2.0
1.0
0.
0.
0.10
0.20
0.30
a/b
$\bar{\mathcal{G}}_T/(M_x^{\infty 2}/b^2h^3)$
b=2 in., h=0.25 in.
Delamination (Center) at y=h
[45/-45/-45/45] Graphite-Epoxy

Fig. 14

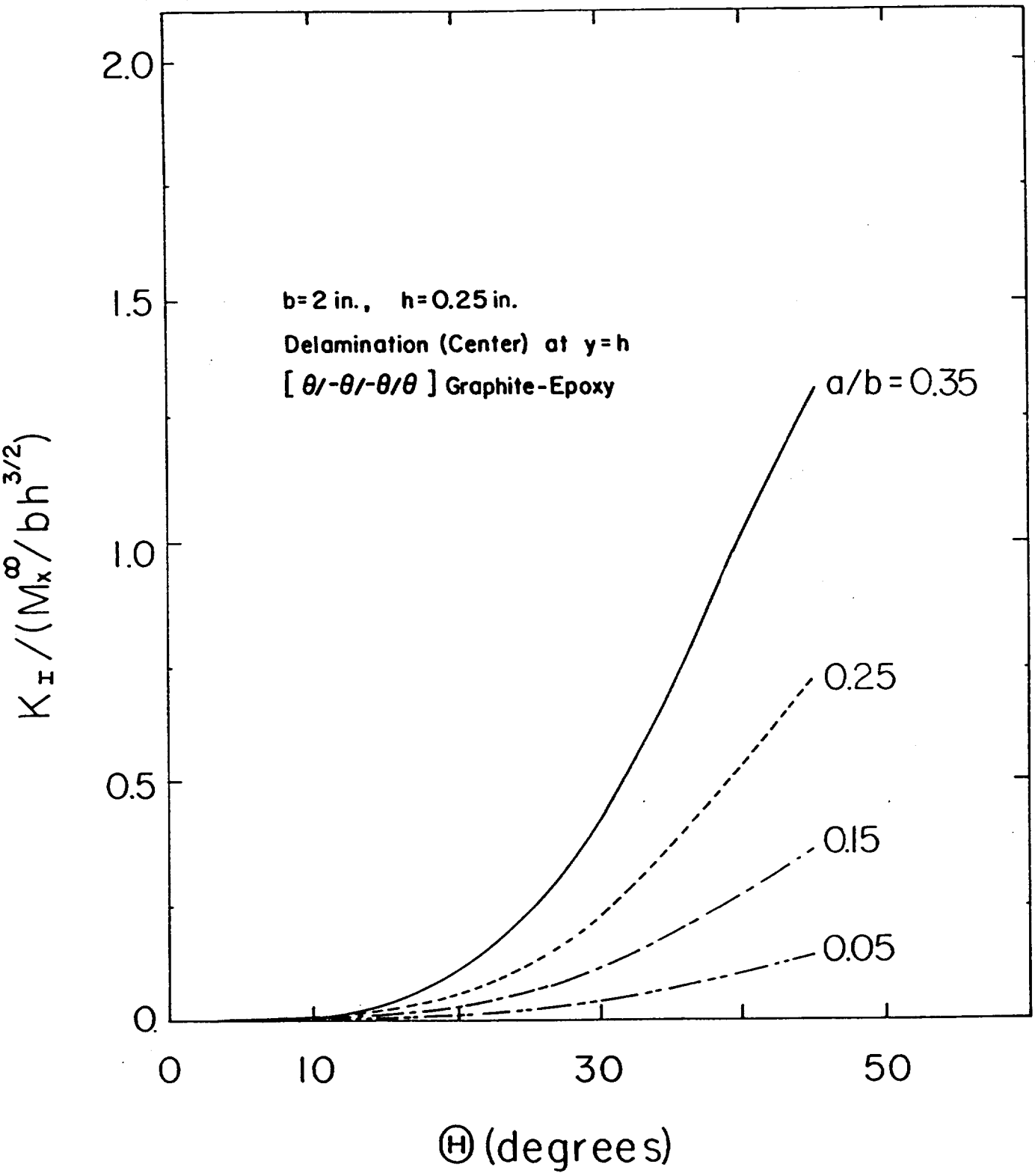
2.0
1.5
1.0
0.5
0
0
10
30
50
b=2 in., h=0.25 in.
Delamination (Center) at y=h
[θ/-θ/-θ/θ] Graphite-Epoxy
a/b = 0.35
0.25
0.15
0.05
$K_I/(M_x^\infty/bh^{3/2})$
Θ (degrees)

Fig. 15